

Surface solitons in waveguide arrays: Analytical solutions

Y. Kominis, A. Papadopoulos and K. Hizanidis

School of Electrical and Computer Engineering, National Technical University of Athens,
Zographou GR-15773, Athens, Greece

gkomin@central.ntua.gr

Abstract: A novel phase-space method is employed for the construction of analytical stationary solitary waves located at the interface between a periodic nonlinear lattice of the Kronig-Penney type and a linear or nonlinear homogeneous medium as well as at the interface between two dissimilar nonlinear lattices. The method provides physical insight and understanding of the shape of the solitary wave profile and results to generic classes of localized solutions having either zero or nonzero semi-infinite backgrounds. For all cases, the method provides conditions involving the values of the propagation constant of the stationary solutions, the linear refractive index and the dimensions of each part in order to assure existence of solutions with specific profile characteristics. The evolution of the analytical solutions under propagation is investigated for cases of realistic configurations and interesting features are presented such as their remarkable robustness which could facilitate their experimental observation.

© 2007 Optical Society of America

OCIS codes: (190.4350) Nonlinear optics at surfaces; (190.4420) Nonlinear optics, transverse effects in; (190.5530) Pulse propagation and temporal solitons; (240.6690) Surface waves.

References and links

1. A. Zangwill, *Physics at Surfaces* (Cambridge University Press, Cambridge, 1988).
2. R. de L. Kronig and W. G. Penney, "Quantum Mechanics of Electrons in Crystal Lattices," *Proc. R. Soc. London* **130**, 499–513 (1930).
3. I. Tamm, *Phys. Z. Sowjetunion* **1**, 733–746 (1932).
4. W. Shockley, "On the Surface States Associated with a Periodic Potential," *Phys. Rev.* **56**, 317–323 (1939).
5. D. Kossel, "Analogies between thin-film optics and electron. band theory of solids," *J. Opt. Soc. Am.* **56**, 1434 (1966).
6. J. A. Arnaud and A. A. Saleh, "Guidance of surface waves by multilayer coatings," *Appl. Opt.* **13**, 2343 (1974).
7. P. Yeh, A. Yariv, and A. Y. Cho, "Optical surface waves in periodic layered media," *Appl. Phys. Lett.* **32**, 104–105 (1978).
8. W. Ng, P. Yeh, P. C. Chen, and A. Yariv, "Optical surface waves in periodic layered medium grown by liquid phase epitaxy," *Appl. Phys. Lett.* **32**, 370–371 (1978).
9. W. L. Barnes, A. Dereux, and T. W. Ebbesen, "Surface plasmon sub-wavelength optics," *Nature* **424**, 824–830 (2003).
10. D. Artigas and L. Torner, "Dyakov Surface Waves in Photonic Metamaterials," *Phys. Rev. Lett.* **94**, 013901 (2005).
11. W. J. Tomlinson, "Surface wave at a nonlinear interface," *Opt. Lett.* **5**, 323–325 (1980).
12. V. K. Fedyanin and D. Mihalache, "P-polarized nonlinear surface polaritons in layered structures," *Z. Phys. B* **47**, 167–173 (1982).
13. N. N. Akhmediev, V. I. Korneev, and Y. V. Kuzmenko, "Excitation of nonlinear surface waves by Gaussian light beams," *Sov. Phys. JETP* **61**, 62–67 (1985).
14. U. Langbein, F. Lederer, and H. E. Ponath, "A new type of non-linear slab-guided waves," *Opt. Commun.* **46**, 167–169 (1983).

15. C. T. Seaton, J. D. Valera, R. L. Shoemaker, G. I. Stegeman, J. T. Chilwell, and S. D. Smith, "Calculations of nonlinear TE waves guided by thin dielectric films bounded by nonlinear media," *IEEE J. Quantum Electron.* **21**, 774–783 (1985).
16. D. Mihalache, G. I. Stegeman, C. T. Seaton, E. M. Wright, R. Zaroni, A. D. Boardman, and T. Twardowski, "Exact dispersion relations for transverse magnetic polarized guided waves at a nonlinear interface," *Opt. Lett.* **12**, 187–189 (1987).
17. D. Mihalache, M. Bertolotti, and C. Sibilia, "Nonlinear wave propagation in planar structures," *Prog. Opt.* **27**, 229–313 (1989).
18. A. D. Boardman, P. Egan, F. Lederer, U. Langbein, and D. Mihalache, *Nonlinear Surface Electromagnetic Phenomena*, edited by H. E. Ponath and G. I. Stegeman, North-Holland, Amsterdam, **29**, 73 (1991).
19. D. N. Christodoulides and R. I. Joseph, "Discrete self-focusing in nonlinear arrays of coupled waveguides," *Opt. Lett.* **13**, 794–796 (1988).
20. A. A. Sukhorukov, Y. S. Kivshar, H. S. Eisenberg, and Y. Silberberg, "Spatial optical solitons in waveguide arrays," *IEEE J. Quantum Electron.* **39**, 31–50 (2003).
21. J. W. Fleischer, G. Bartal, O. Cohen, T. Schwartz, O. Manela, B. Freedman, M. Segev, H. Buljan and N. K. Efremidis, "Spatial photonics in nonlinear waveguide arrays," *Opt. Express* **13**, 1780–1796 (2005).
22. S. Trillo and W. Torruellas (Eds.), *Spatial Solitons* (Springer-Verlag, Berlin, 2001).
23. K. G. Makris, S. Suntsov, D. N. Christodoulides, G. I. Stegeman, and A. Hache, "Discrete surface solitons," *Opt. Lett.* **30**, 2466–2468 (2005).
24. S. Suntsov, K. G. Makris, D. N. Christodoulides, G. I. Stegeman, A. Hache, R. Morandotti, H. Yang, G. Salamo, and M. Sorel, "Observation of discrete surface solitons," *Phys. Rev. Lett.* **96**, 063901 (2005).
25. M. I. Molina, I. L. Garanovich, A. A. Sukhorukov, and Y. S. Kivshar, "Discrete surface solitons in semi-infinite binary waveguide arrays," *Opt. Lett.* **31**, 2332–2334 (2006).
26. M. I. Molina, R. A. Vicencio, and Y. S. Kivshar, "Discrete solitons and nonlinear surface modes in semi-infinite waveguide arrays," *Opt. Lett.* **31**, 1693–1695 (2006).
27. D. Mihalache, D. Mazilu, F. Lederer, and Y. S. Kivshar, "Stable discrete surface light bullets," *Opt. Express* **15**, 589–595 (2007).
28. M. Stepic, E. Smirnov, C. E. Ruter, D. Kip, A. Maluckov, and L. Hadzievski, "Tamm oscillations in semi-infinite nonlinear waveguide arrays," *Opt. Lett.* **32**, 823–825 (2007).
29. Y. V. Kartashov, V. A. Vysloukh, and L. Torner, "Surface gap solitons," *Phys. Rev. Lett.* **96**, 073901 (2006).
30. C. R. Rosberg, D. N. Neshev, W. Krolikowski, A. Mitchell, R. A. Vicencio, M. I. Molina, and Y. S. Kivshar, "Observation of surface gap solitons in semi-infinite waveguide arrays," *Phys. Rev. Lett.* **97**, 083901 (2006).
31. E. Smirnov, M. Stepic, C. E. Ruter, D. Kip, and V. Shandarov, "Observation of staggered surface solitary waves in one-dimensional waveguide arrays," *Opt. Lett.* **31**, 2338–2340 (2006).
32. K. G. Makris, J. Hudock, D. N. Christodoulides, G. I. Stegeman, O. Manela, and M. Segev, "Surface lattice solitons," *Opt. Lett.* **31**, 2774–2776 (2006).
33. M. I. Molina and Y. S. Kivshar, "Interface localized modes and hybrid lattice solitons in waveguide arrays," *Phys. Lett. A* **362**, 280–282 (2007).
34. Y. V. Kartashov, V. A. Vysloukh, D. Mihalache, and L. Torner, "Generation of surface soliton arrays," *Opt. Lett.* **31**, 2329–2331 (2006).
35. Y. V. Kartashov, and L. Torner, "Multipole-mode surface solitons," *Opt. Lett.* **31**, 2172–2174 (2006).
36. X. Wang, A. Bezryadina, Z. Chen, K. G. Makris, D. N. Christodoulides and G. I. Stegeman, "Observation of two-dimensional surface solitons," *Phys. Rev. Lett.* **98**, 123903 (2007).
37. A. Szameit, Y. V. Kartashov, F. Dreisow, T. Pertsch, S. Nolte A. Tunnermann, and L. Torner, "Observation of two-dimensional surface solitons in asymmetric waveguide arrays," *Phys. Rev. Lett.* **98**, 173903 (2007).
38. Y. V. Kartashov, F. Ye, and L. Torner, "Vector mixed-gap surface solitons," *Opt. Express* **14**, 4808–4814 (2006).
39. I. L. Garanovich, A. A. Sukhorukov, Y. S. Kivshar, and M. Molina, "Surface multi-gap vector solitons," *Opt. Express* **14**, 4780–4785 (2006).
40. Y. V. Kartashov, V. A. Vysloukh, and L. Torner, "Surface lattice kink solitons," *Opt. Express* **14**, 12365–12372 (2006).
41. Y. V. Kartashov, V. A. Vysloukh, A. A. Egorov and L. Torner, "Surface vortex solitons," *Opt. Express* **14**, 4049–4057 (2006).
42. K. Motzek, A. A. Sukhorukov, and Y. S. Kivshar, "Self-trapping of polychromatic light in nonlinear periodic photonic structures," *Opt. Express* **14**, 9873–9878 (2006).
43. K. Motzek, A. A. Sukhorukov, and Y. S. Kivshar, "Polychromatic interface solitons in nonlinear photonic lattices," *Opt. Lett.* **31**, 3125–3127 (2006).
44. A. A. Sukhorukov, D. N. Neshev, A. Dreischuh, R. Fischer, S. Ha, W. Krolikowski, J. Bolger, A. Mitchell, B. J. Eggleton, and Y. S. Kivshar, "Polychromatic nonlinear surface modes generated by supercontinuum light," *Opt. Express* **14**, 11265–11270 (2006).
45. G. A. Siviloglou, K. G. Makris, R. Iwanow, R. Schiek, D. N. Christodoulides, and G. I. Stegeman, "Observation of discrete quadratic surface solitons," *Opt. Express* **14**, 5508–5516 (2006).
46. Y. V. Kartashov, L. Torner, and V. A. Vysloukh, "Lattice-supported surface solitons in nonlocal nonlinear media,"

- Opt. Lett. **31**, 2595–2597 (2006).
47. Y. Kominis, "Analytical solitary wave solutions of the nonlinear Kronig-Penney model in photonic structures," *Phys. Rev. E* **73**, 066619 (2006).
 48. Y. Kominis and K. Hizanidis, "Lattice solitons in self-defocusing optical media: analytical solutions of the nonlinear Kronig-Penney model," *Opt. Lett.* **31**, 2888–2890 (2006).
 49. N. Akhmediev, A. Ankiewicz, and R. Grimshaw, "Hamiltonian-versus-energy diagrams in soliton theory," *Phys. Rev. E* **59**, 6088–6096 (1999).
 50. A. Ankiewicz and N. Akhmediev, "Stability analysis for solitons in planar waveguides, fibres and couplers using Hamiltonian concepts," *IEE Proc.-Optoelectron.* **150**, 519–526 (2003).
-

1. Introduction

Surface waves appear in diverse areas of physics, chemistry, biology, and display properties that have no counterpart in the bulk [1]. Surface waves have been originally considered in the context of solid state and condensed matter physics, where a Kronig-Penney model [2] was introduced to demonstrate the band structure of electronic states in crystals. This model has been used by Tamm [3] who showed that at a semi-infinite Kronig-Penney potential, the formation of surface states (also known as Tamm states) is possible under certain conditions, while the case of a more general one-dimensional potential was examined by Shockley [4].

In linear optics, the utilization of periodic layered media in guided wave optical applications has been a subject of theoretical and experimental investigations for a few decades. Among these studies of particular interest is the investigation of the wave guiding properties of the interface between such a periodic medium and a homogeneous medium and the formation of the surface waves. The existence of electromagnetic surface waves was suggested by Kossel [5] and Arnaud [6] and successfully observed in AlGaAs multilayer structures [7, 8]. Also, such waves were shown to exist at metal-dielectric interfaces [9] (plasmon waves) as well as at the interfaces of anisotropic materials [10].

In nonlinear optics TE, TM and mixed-polarization surface waves, traveling along the single interface between homogeneous dielectric media, has been theoretically predicted and analyzed in several works [11, 12, 13, 14, 15, 16, 17, 18] and the formation of surface states has been shown for cases where no linear states exist. However, the observation of such waves has been hindered by experimental difficulties mainly related to high power thresholds required for proper excitation. However, the recent studies of solitary wave formation in nonlinear periodic lattices [19, 20, 21, 22] have shown that the combination of nonlinearity and periodicity allows for overcoming the experimental limitations of the homogeneous cases. The latter resulted in the recent renewal of the interest for the study of surface waves in the interfaces of such photonic structures. The formation of surface solitons was predicted and almost directly observed in 2006 for the cases of discrete surface solitons [23, 24, 25, 26, 27, 28] and surface gap solitons [29, 30, 31]. Moreover, surface lattice solitons have been theoretically predicted for the case of the heterointerface between two different semi-infinite waveguide arrays [32, 33], as well as at the boundaries of two-dimensional nonlinear lattices [32, 34, 35, 36, 37]. It has been shown that, as in the case of bulk and lattice solitons, vector [38, 39], kink [40] and vortex [41] surface solitons can exist. Finally, polychromatic surface modes have been studied and experimentally observed [42, 43, 44], while formation of surface lattice solitons has been reported for the case of quadratic [45] and nonlocal nonlinear media [46].

In this work we present a phase space method for the construction of analytical solitary wave solutions located at the interface of a nonlinear (Kerr) Kronig-Penney lattice with a homogeneous linear or nonlinear medium as well as at the interface between two dissimilar nonlinear lattices. This novel class of solutions is obtained under quite generic conditions, while the method is applicable to a large variety of systems, including more complex geometries consisting of linear/nonlinear, self-focusing/defocusing and homogeneous/periodic parts, while other

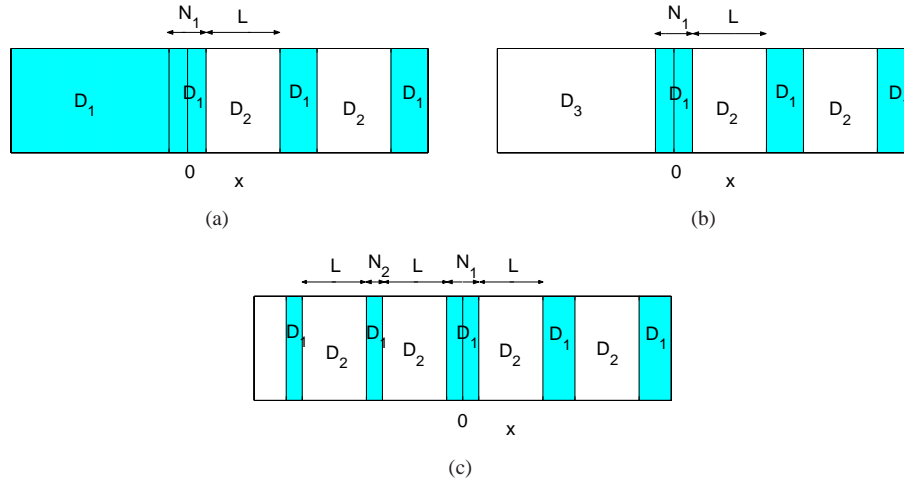


Fig. 1. Transverse profile of the photonic structure consisting of a nonlinear lattice (parts D_1 and D_2) and a homogeneous linear (a) or nonlinear (b) homogeneous medium (part D_3) as well as two dissimilar nonlinear lattices having different widths of the corresponding nonlinear parts (c). Shaded areas denote nonlinear medium while nonshaded areas denote linear medium.

types of nonlinearity can also be examined. The method has been also used for providing analytical solutions for solitary waves in infinite self-focusing [47] and self-defocusing [48] lattices.

2. Construction of analytical stationary solutions

We consider the case of a realistic model described by the Nonlinear Schrodinger (NLS) equation with piecewise-constant coefficients, namely a nonlinear Kronig-Penney type of model:

$$i \frac{\partial \psi}{\partial z} + \frac{\partial^2 \psi}{\partial x^2} + \varepsilon(x) \psi + g(x) |\psi|^2 \psi = 0 \quad (1)$$

where z , x and ψ are the normalized propagation distance, transverse dimension and electric field, respectively. The transverse variation of the linear refractive index is given by $\varepsilon(x)$, while the spatial dependence of the nonlinear refractive index is provided through $g(x)$. The stationary solutions of (1) have the form $\psi(x, z) = u(x; \beta) e^{i\beta z}$, and satisfy the nonlinear ordinary differential equation

$$\frac{d^2 u}{dx^2} + [\varepsilon(x) - \beta] u + g(x) u^3 = 0 \quad (2)$$

where β is the propagation constant and $u(x; \beta)$ is the real transverse wave profile. Equation (2) describes a nonautonomous nonlinear dynamical system which is in general nonintegrable. Solitary waves correspond to solutions of infinite period, asymptotically tending to saddle points of the phase space. Such solutions are mostly located in chaotic areas of the phase space, due to the presence of homoclinic (or heteroclinic) chaos, resulting in a complex transverse profile for the stationary solitary wave. However, as we show in the following, specific values of the propagation constant β result in integrability of the system in the sense of global bifurcations, and allow for the construction of analytical solutions.

We consider the case of a photonic structure consisting of two parts: either a nonlinear lattice and a homogeneous (linear or nonlinear) medium or two dissimilar nonlinear lattices having

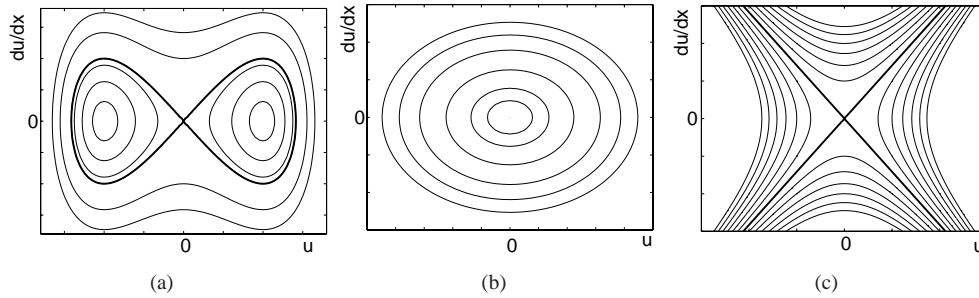


Fig. 2. Phase space for each part of the structure: (a) nonlinear part (D_1) for $\beta > \varepsilon_1$, (b) linear part (D_2 or D_3) for $\beta < \varepsilon_i$ ($i = 2$ or 3) and, (c) linear part (D_2 or D_3) for $\beta > \varepsilon_i$ ($i = 2$ or 3).

different widths of the corresponding nonlinear parts. The geometry of the configurations is shown in Fig. 1. The functions $\varepsilon(x)$ and $g(x)$ are defined as follows

$$(\varepsilon(x), g(x)) = \begin{cases} (\varepsilon_1, 2), & x \in D_1 \\ (\varepsilon_2, 0), & x \in D_2 \\ (\varepsilon_3, 0), & x \in D_3 \end{cases} \quad (3)$$

In each part eq. (2) is integrable with corresponding phase spaces such as those shown in Fig. 2. The phase space corresponding to the nonlinear part is shown in Fig. 2(a), for the case $\beta > \varepsilon_1$, where a homoclinic solution exist. For a linear part the phase space is shown in Fig. 2(b) and (c) for $\beta < \varepsilon_i$ and $\beta > \varepsilon_i$ ($i = 2$ or 3), respectively. The stationary solutions of (2) can be provided by composing solutions of these systems, which have matched conditions for u and its derivative, at the interfaces. As shown in [47], for a propagation constant

$$\beta_n = \varepsilon_2 - \left(\frac{n\pi}{L}\right)^2, \quad n = 1, 2, \dots \quad (4)$$

corresponding to the case where an integer number of half-periods of the solution in the linear part (D_2) is contained in the length L , the continuity conditions are met simultaneously in all boundaries, for $x > 0$: Any solution of (2) starting from a point of the homoclinic orbit inside the nonlinear part (D_1) at some x , returns to the homoclinic orbit after evolving in the linear part (D_2) and subsequently evolves again according to the homoclinic orbit. Thus, the solution approaches the origin asymptotically as $x \rightarrow +\infty$, moving on the homoclinic orbit but interrupted periodically due to the linear part of the structure. For the case of a nonlinear homogeneous part (Fig. 1(a)) [for simplicity we consider that the medium characteristics are identical with those of the nonlinear part of the lattice (D_1)], the solution moves on the same homoclinic orbit for $x < -N_1/2$, approaching the origin as $x \rightarrow -\infty$ (Fig. 3(a)). The resulting solutions form a family, parameterized by the position of the maximum of the homoclinic orbit x_0 , corresponding to solitary wave profiles zero asymptotic values. For the case of a linear homogeneous medium (Fig. 1(b)) we can distinguish two different cases depending on the value of the propagation constant β with respect to the value of the linear refractive index ε_3 : (i) For a $\beta < \varepsilon_3$ any solution (for every x_0) constructed in the aforementioned way for the lattice part of the structure meets at $x = -N_1/2$ one of the elliptical curves of the phase space shown in Fig. 2(b) and then evolves periodically for $x \in [-N_1/2, -\infty)$ (Fig. 3(b)). This family of solutions correspond to solitary wave profiles with a zero asymptotic value for $x \rightarrow +\infty$ and

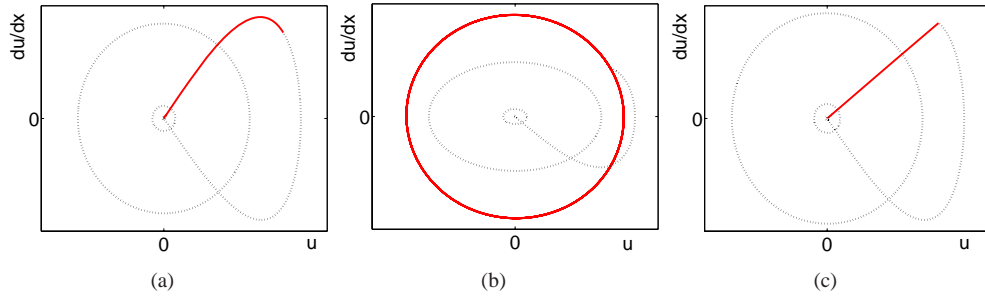


Fig. 3. Phase space representation of the constructed solutions for n even. (a) Nonlinear homogeneous part, (b) Linear homogeneous part having $\beta < \varepsilon_3$, and (c) Linear homogeneous part having $\beta > \varepsilon_3$. Dotted line denotes the solution in the lattice part and solid line denotes the solution in the homogeneous part.

a finite periodic (sinusoidal) pedestal for $x \rightarrow -\infty$. (ii) For every $\beta > \varepsilon_3$ there exist a solution (for a particular x_0) for which the part of the homoclinic orbit comprising the lattice part of the solution in $x \in [-N_1/2, N_1/2]$ intersects one of the straight lines tending to the origin as $x \rightarrow +\infty$ of the phase space shown in Fig. 2(c) (this having $u > 0$, without loss of generality), at the boundary $x = -N_1/2$. This solution correspond to a solitary wave profile with zero asymptotic values (Fig. 3(c)). Finally, for the case of two dissimilar lattices (Fig. 1(c)), the solution evolves in the the left lattice, similarly to the right lattice, tending to the origin as $x \rightarrow -\infty$. Note that in Fig. 3, the case of an even n is shown, so that the solution in the lattice part lays on a single branch of the homoclinic; in the case of n odd, the solution in the lattice part lays on both branches of the homoclinic [47].

In all cases, the solitary wave stationary solutions corresponding to β_n can be given analytically in the following form

$$u(x; \beta_n, x_0) = \begin{cases} v(x; \beta_n, x_0) & x \in D_1 \\ a_k \sin(\sqrt{\varepsilon_{2,3} - \beta_n}x + \phi_k) & x \in D_2, D_3 \end{cases} \quad (5)$$

where $v(x; \beta, x_0) = \pm \sqrt{\beta - \varepsilon_1} \operatorname{sech}(\sqrt{\beta - \varepsilon_1}(x - x_0))$ is the homoclinic solution of the nonlinear part (D_1) of the structure (Fig. 2(a)), and (a_k, ϕ_k) are directly obtained from the continuity conditions of u and its derivative at the interfaces.

3. Results and discussion

In the following we apply the phase space method for the construction of surface localized solutions for the case of a lattice having a linear refractive index profile with parameters $\varepsilon_1 = 0$, $\varepsilon_2 = 0.3$, $N_1 = 2\pi$, $L = 4\pi$. For this case the condition for the existence of the aforementioned family of solutions ($\varepsilon_1 < \beta < \varepsilon_2$) are met for propagation constants β_n given by eq. (4) for $n = 1, 2$. Each one of these values β_n is located in a different finite gap of the linear band structure of the infinite lattices [47], as shown in Fig. 4. The normalized propagation distance $z_{max} = 100$, used in the numerical simulations, corresponds to an actual propagation length of $10.7 - 24.3mm$, for the case of a nonlinear material of AlGaAs type, and $22.3 - 50mm$ for the case of LiNbO₃, when the transverse coordinate is normalized to $X_0 = 2 - 3\mu m$. The numerical simulations of the propagation of the analytically obtained stationary solutions have been performed utilizing a standard beam propagation method. A noise level of the order of 10^{-2} (with respect to the maximum of the corresponding solution) has been superimposed to the stationary solutions, in order to investigate their stability.

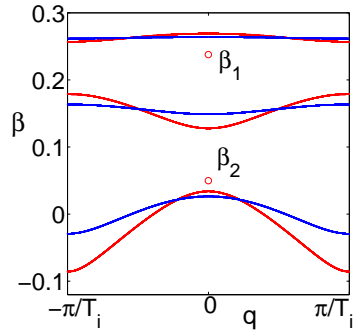


Fig. 4. Band structure of the linearized system (propagation constant β vs Bloch wave number q) for the two lattices having $\varepsilon_1 = 0$, $\varepsilon_2 = 0.3$, $L = 4\pi$ and $N_1 = 2\pi$ (blue line), $N_2 = \pi$ (red line). $T_i = L + N_i$, $i = 1, 2$ is the period of each lattice. Circles depict the location of the analytically obtained localized modes for $n = 1, 2$.

3.1. Nonlinear homogeneous medium

We consider the case where the nonlinear homogeneous medium has the same material characteristics with the nonlinear part of the lattice. In this case there exist an infinite number of solutions corresponding to different x_0 for each β_n . The phase space representation of a typical solution is shown in Fig. 3(a), while their profiles for some characteristic cases of x_0 are shown in Fig. 5. Solitary wave profiles can attain their maximum amplitude inside the homogeneous medium (Figs. 5(left)), in the linear part of the lattice (Figs. 5(middle)), or in the first nonlinear part of the lattice (Figs. 5(right)).

The propagation of the analytically obtained solitary wave profiles of Fig. 5 is illustrated in Fig. 6. It is shown that the solutions corresponding to $n = 1$ (Figs. 6(top)), under propagation, break in two parts: one traveling inside the homogeneous part and one which is localized close to the interface. The latter corresponds to a surface mode having different x_0 and/or β . Such mode transformations are characterized by evolution of an initial mode to a more stable mode having lower values of Hamiltonian and Energy [49, 50]: the initial solution emits part of its energy as a wave traveling inside the homogeneous energy, in order to evolve to the new localized mode. It is remarkable that this transformation process can be quite slow (Fig. 6(top, right)), and become apparent for large propagation distances. Depending on the length of an actual experimental configuration some these cases can also be considered as robust, since the laminar propagation distance can be larger than the actual propagation length. Also, the mode transformation process itself can also be potentially useful in applications. On the other hand, as shown in Fig. 6(bottom) the solutions corresponding to $n = 2$ are remarkably stable.

3.2. Linear homogeneous medium

In this case we consider a homogeneous linear medium having $\varepsilon_3 = 0.1$. For the formation of surface waves in the interface between the lattice and a linear homogeneous medium, we can distinguish between two qualitatively different cases:

3.2.1. Case: $\beta < \varepsilon_3$

In this case, for each β_n there exist a infinite number of solutions, characterized by a different x_0 . Their phase space representation has been shown in Fig. 3(b) and their profiles for some characteristic values of x_0 are shown in Fig. 7(bottom), corresponding to $n = 2$, for which

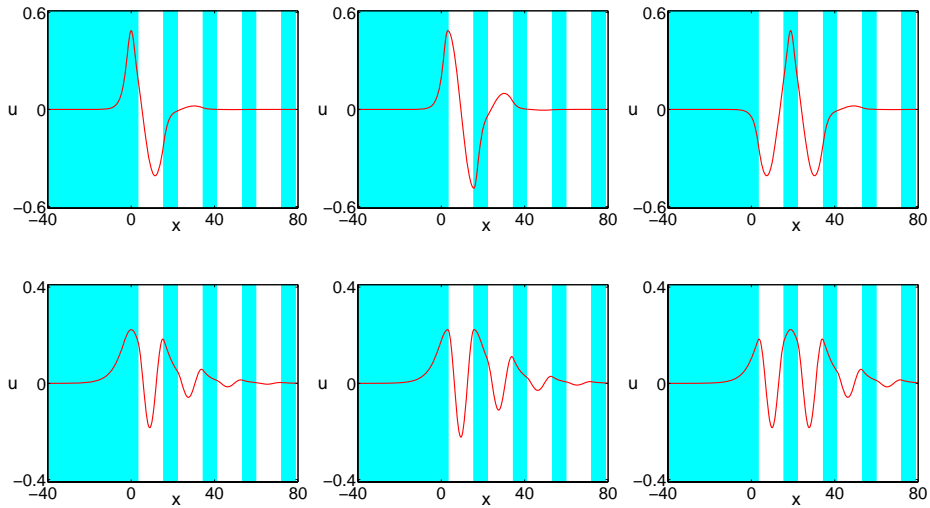


Fig. 5. Profiles of stationary surface lattice solutions for the case of a nonlinear homogeneous medium having the same material characteristics with the nonlinear part of the lattice, for $n = 1, 2$ (top to bottom) and $x_0 = 0, \pi, 2\pi$ (left to right).

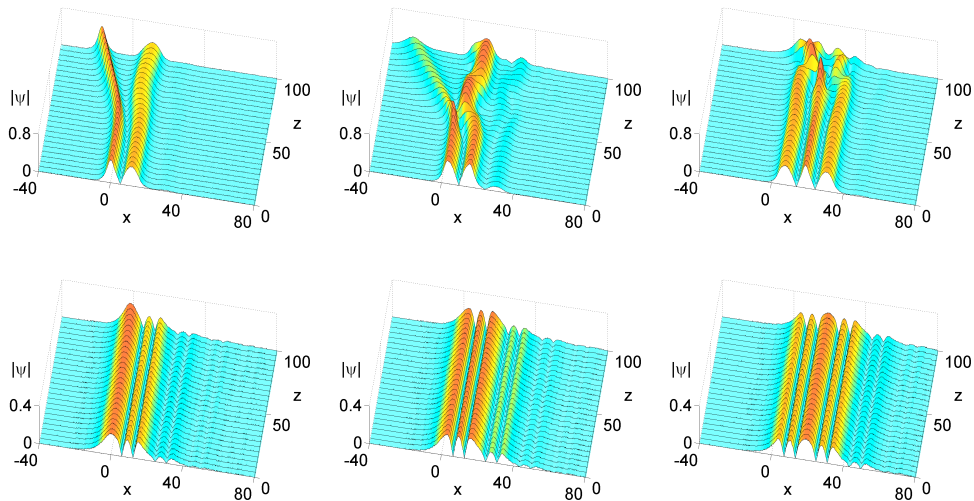


Fig. 6. Propagation of the stationary solutions shown in Fig. 5.

$\beta_2 < \epsilon_3$ (for the specific values of the linear refractive indices used in our example). It is shown that for $x_0 \in [-N_1/2, N_1/2]$ the maximum of the solution is located inside the first nonlinear waveguide while the amplitude of the periodic pedestal in the linear homogeneous medium decreases as x_0 moves from the left boundary of the nonlinear part to the right. An increasing width of the nonlinear part N_1 would also result in decreasing pedestal. Also, solutions having their maxima located in other than the first nonlinear waveguide, can be constructed. Figure 8(bottom) shows a stable evolution of these stationary solutions under propagation.

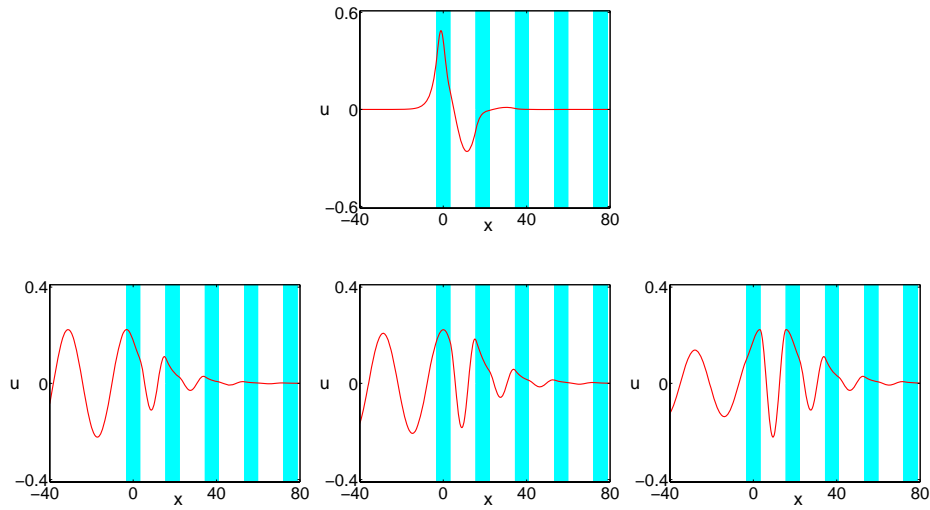


Fig. 7. Profiles of stationary surface lattice solutions for the case of a linear homogeneous medium having $\varepsilon_3 = 0.1$, for $n = 1, 2$ (top to bottom) and $x_0 = -\pi, 0, \pi$ (left to right).

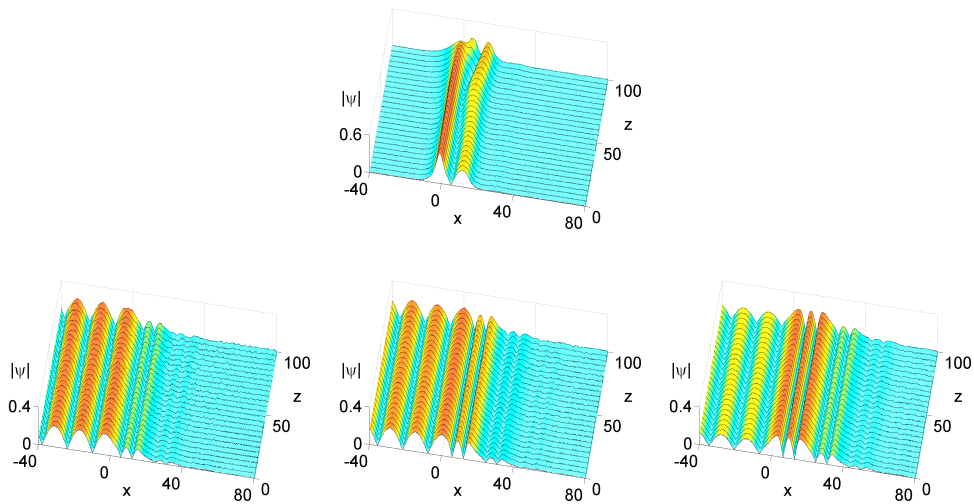


Fig. 8. Propagation of the stationary solutions shown in Fig. 7.

3.2.2. Case: $\beta > \varepsilon_3$

In this case, for each value of β_n , there exist one solution for a particular x_0 , given by

$$x_0 = \frac{1}{\sqrt{\beta - \varepsilon_1}} \operatorname{sech}^{-1} \left(\frac{\sqrt{\varepsilon_3 - \varepsilon_1}}{\sqrt{\beta - \varepsilon_1}} \right) - \frac{N_1}{2} \quad (6)$$

The phase space representation of the solutions is shown in Fig. 3(c). For our example, this case corresponds to $n = 1$. The profile of such a solution is shown in Figs. 7(top), while its propagation is illustrated in Figs. 8(top), where a large distance of laminar propagation is shown, with the part in the right slightly moving to the right for $z > 60$.

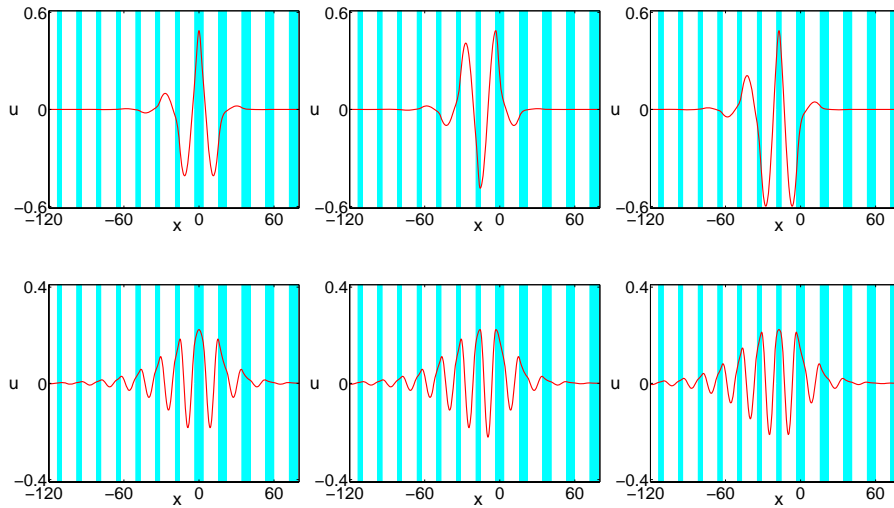


Fig. 9. Profiles of stationary surface lattice solutions for the case of the interface between two dissimilar nonlinear waveguide arrays, for $n = 1, 2$ (top to bottom), and $x_0 = 0, -\pi, -3\pi/2$ (left to right).

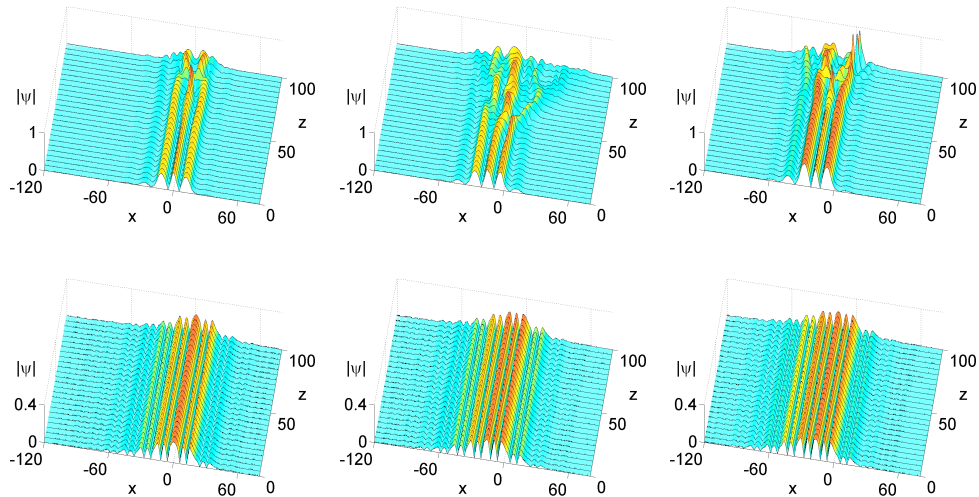


Fig. 10. Propagation of the stationary solutions shown in Fig. 9.

3.3. Two dissimilar nonlinear waveguide arrays

We consider the configuration shown in Fig. 1(c), with $N_2 = \pi$. The profiles of the analytically obtained solutions are shown in Fig. 9, for the case where the maximum of the solution is located at the center of the first nonlinear part of the right lattice ($x_0 = 0$), at the linear part between the two lattices ($x_0 = -\pi$) and at the center of the first nonlinear part of the left lattice ($x_0 = -3\pi/2$). It is shown that the solitary wave is more extended inside the array with the narrower nonlinear part. The propagation of these solutions is shown in Fig. 10, with the solutions corresponding to $n = 2$ (Fig. 10(bottom)), having stable evolution under propagation. Note that

the values of the propagation constants $\beta_{1,2}$ corresponding to the analytically obtained solutions are located within the finite band gaps of both lattices, as shown in Fig. 4.

4. Summary and conclusions

A novel method for the construction of analytical stationary solutions of surface lattice solitary waves in waveguide arrays has been presented. The method is based on the phase space geometry of the underlying dynamical system describing the profiles of the stationary solutions. The applicability of the method to configurations consisting of semi-infinite lattices and linear or nonlinear homogeneous parts as well as two dissimilar lattices has been shown. Several classes of analytical solutions having qualitatively different characteristics have been obtained, including families of localized solutions on zero background as well as novel families of localized solutions having a semi-infinite periodic pedestal. The method provides physical insight for the appropriate selection of parameters for the formation of each family of solutions. Moreover, the analytically obtained solutions can serve as the basis for further investigations of the configurations considered in this work as well similar ones, either in the context of analytical perturbation methods or numerical continuation methods. It is worth mentioning that the method is similarly applicable for the case of self-defocusing nonlinearities [48], while a wide range of geometries can be treated, including also the presence of defects. Finally, the propagation of the analytically obtained solutions of this work, has been numerically investigated and cases of stable propagation were shown for realistic configurations, therefore facilitating their experimental observation.

Acknowledgments

Y.K. and K.H. acknowledge funding by the European Social Fund (75%) and National Resources (25%)-Operational Program for Educational and Vocational Training II (EPEAEK II) and particularly the Program PYTHAGORAS. A.P. acknowledges funding by the project PENED 2003; the project is cofinanced 75% of public expenditure through EC - European Social Fund 25% of public expenditure through Ministry of Development - General Secretariat of Research and Technology and through private sector, under measure 8.3 of OPERATIONAL PROGRAMME "COMPETITIVENESS" in the 3rd Community Support Programme.